Applied Geochemistry 163 (2024) 105937

Contents lists available at ScienceDirect

Applied Geochemistry

journal homepage: www.elsevier.com/locate/apgeochem

Modelling CO_2 recycling to the atmosphere after CO_2 sequestration with ground basalt

Michael O. Schwartz

MathGeol, Postfach, 101204, 30833, Langenhagen, Germany

ARTICLE INFO

Editorial handling by: Dr Lauren E Beckingham

Keywords:
Climate change
Carbon dioxide
CO_2
Basalt fertilizer
Numerical model

ABSTRACT

Ground basalt mixed with agricultural fertilizer acts as a sink for atmospheric carbon dioxide (CO_2). The constituents of dissolving basalt form carbonate minerals through reaction with aqueous carbon species. The carbonate minerals start dissolving towards the end of the basalt dissolution process, leading to an increase in the CO_2 partial pressure (p_{CO2}) of the soil pore fluid. The pathway of possible recycling to the atmosphere of originally sequestered CO_2 is via recycling to surface waters degassing CO_2. This process is controlled by various variables, the most important being (1) the pH and dissolved carbon concentration of the infiltrating pore fluids and (2) the degree of CO_2 supersaturation of the water courses that receive the pore fluids with increased p_{CO2}. The CO_2 recycling rate decreases with increasing degree of supersaturation of the surface waters. CO_2 is less likely to be recycled to the atmosphere if the surface water–atmosphere system of the receiving streams favours supersaturation. The modelled CO_2 recycling fraction is in the range of 0.34–1 for the individual mean p_{CO2} of the world's major rivers (1070–4350 ppm_v). Taking the mean p_{CO2} of 47 large rivers worldwide (3200 ppm_v) as a reference, the recycled fraction is in the range of 0.34–0.43.

1. Introduction

In terms of CO_2 sequestration potential, basalt is unique. Basalt is both a highly reactive and wide-spread silicate rock. Ground basalt added to agricultural fertilizer captures atmospheric carbon dioxide (CO_2), raises the soil pH, reduces ocean acidification and supplies important nutrients such as magnesium, potassium, calcium, iron and phosphorus. Ground silicate rock has been used as mineral fertilizer since the early thirties (Hilf, 1938; de Villiers, 1961; Gillman et al., 2002; van Straaten, 2006; Anda et al., 2009). More recently, CO_2 sequestration by silicate rock has been investigated by incubation and infiltration experiments with application rates being in the range from 50 to 220 tonnes per hectare (ten Berge, 2012; Dietzen et al., 2018; Kelland et al., 2020; Amann et al., 2020; Vienne et al., 2022). The weathering of silicate rock involves the reaction with dissolved carbon species, the activities of which are controlled by the thermodynamic equilibrium between CO_2 gas in the atmosphere and soil and liquid CO_2. This is a natural process, which controls the CO_2 level of the atmosphere on the geological time scale. The only way to enhance this natural process is to increase the reactive surface area of the silicate rock by grinding. A variety of strategies for implementing enhanced weathering on the global scale have been published (Taylor et al., 2015, 2017; Strefler et al., 2018; Beerling et al., 2020).

The above studies similarly fail to thoroughly address CO_2 recycling to the atmosphere after successful sequestration or do not mention it at all (the majority of papers). To the best of the author's knowledge, CO_2 recycling has not yet been quantified. This paper is the first attempt to define the conditions under which CO_2 recycling takes place. The models are based on an exceptionally large set of empirical data from Brazilian Amazonia (Johnson et al., 2008; Fan and Miguez-Macho, 2010) within the context of global hydrochemical data (Brook et al., 1983; Kessler and Harvey, 2001; Zhang et al., 2017).

The focus on empirical data from Brazil has a useful side effect. Brazil has the highest deforestation rate in the world and is under considerable international pressure to counteract the negative effects of deforestation (Grieger, 2020). Coincidentally, Brazil is well suited for compensation efforts. Brazil has numerous basalt occurrences – a prerequisite for short transport distances (Hartmann and Moosdorf, 2012; Lefebvre et al., 2019). Brazil has a high precipitation rate in large parts of the country – a prerequisite for high CO_2 sequestration rates of basalt-amended fertilizer (Fan and Miguez-Macho, 2010).

E-mail address: mathgeol@yahoo.de.

https://doi.org/10.1016/j.apgeochem.2024.105937
Received 22 February 2023; Received in revised form 10 February 2024; Accepted 18 February 2024
Available online 19 February 2024

Table 1
PHREEQC model set-up.

Simulation period (a)	40–135
Time step (s)	3.942e5 - 1.3134e6
Number of cells (−)	1
Cell length (not variable) (m)	1
Dispersivity (m)	0.0
Diffusion coefficient (m^2/s)	0.0
In-flow boundary condition	Constant flow
Out-flow boundary condition	Constant flow
Porosity (−)	0.3
Grain density (kg/dm^2)	2.8
Reactive surface area of all components except clay minerals (m2/g)	2.47–22.2
Reactive surface area of clay minerals (m^2/g)	7.4–74.0
Dissolution shrinking core exponent (−)	0.67
Initial concentration of precipitating minerals (moles per litre of pores)	0.0009

2. Materials and methods

The geochemical transport model is calculated with the PHREEQC code (Parkhurst and Appelo, 2013; Supplementary Information with exemplary PHREEQC script). Both the dispersivity and diffusion coefficient are set to zero (Table 1). For this special case, the program performs the calculations with a standard cell length of 1 m no matter what cell length is defined in the input file.

The PHREEQC model is based on empirical data from Brazilian Amazonia for the 1979–2007 reference period but can be adapted to other reference periods with quite different recharge rates or other regions. The infiltration rate (I) (see Equation (2) below) is 600, 1200 or 2000 mm/a, approximately corresponding to the Amazonian minimum, median and maximum recharge, respectively of the 1979–2007 reference period (Fan and Miguez-Macho, 2010). For a typical porosity of 0.3, the corresponding pore velocities (infiltration divided by porosity) are 2000, 4000 or 6666 mm/a. To achieve a satisfactory resolution in time, the actual pore velocities and the actual concentrations of solid phases are multiplied by 10. Scoping calculations have shown that both the model with the raw data and the model using the factor 10 are equivalent.

The infiltration rate (I) is assumed to equal recharge (R) (allowing for runoff) plus transpiration (T), which is assumed to account for 57.2% of evapotranspiration (ET) according to a global average (Wei et al., 2017). For the 1979–2007 reference period, the mean R is 787 mm/a, and the mean ET is 1387 mm/a (Fan and Miguez-Macho, 2010). Using these average values, infiltration (I) is calculated according to

$$I = R + (787\text{x}100)R/(1387\text{x}57.2) \quad (1)$$

Table 3
Reactive transport model setup: Initial composition of the soil pore fluid and infiltrating fluid.

	Spring water scenario	Rainwater scenario
	Brazil Amazonia Spring water (Johnson et al., 2008)	Southeastern Brazil rainwater (Oliveira et al., 2012)
pH (−)	4.65	5.8
Al (moles/L)	4.0×10^{-7}[a]	4.0×10^{-7}
C (moles/L)	1.87×10^{-3}	1.0×10^{-3}[b]
Ca (moles/L)	1.22×10^{-5}	7.4×10^{-6}
Cl (moles/L)	1.1×10^{-5}[a]	1.1×10^{-5}
Fe (moles/L)	6.6×10^{-8}[a]	6.6×10^{-8}
K (moles/L)	3.84×10^{-5}	3.0×10^{-6}
Mg (moles/L)	2.47×10^{-5}	7.0×10^{-7}
Na (moles/L)	4.26×10^{-5}	3.6×10^{-6}
Si (moles/L)	1.8×10^{-7}[a]	1.8×10^{-7}

[a] Southeastern Brazil rainwater (Oliveira et al., 2012).
[b] Calculated for mean CO_2 partial pressure in Brazil Amazonia soil at 0.1–0.5 m depth (Johnson et al., 2008).

Table 2
Reactive transport model setup: Initial weight fractions, reactive surface areas and kinetic properties.

Mineral/glass	Chemical composition	Initial weight fraction (t/t)	Reactive surface area (m^2/g)
Amorphous SiO_2	SiO_2	0.0[a]	7.4
Illite	$K_{0.85}Si_{3.15}Al_{2.85}O_{10}(OH)_2$	0.0[a]	7.4
Calcite	$CaCO_3$	0.0[a]	7.4
Siderite	$FeCO_3$	0.0[a]	7.4
Magnesite	$MgCO_3$	0.0[a]	7.4
Ca-montmorillonite	$Ca_{0.17}Al_{1.68}Mg_{0.33}Si_{3.99}O_{10}(OH)_2$	0.0[a]	7.4
Na-montmorillonite	$Na_{0.33}Al_{1.67}Mg_{0.33}Si_4O_{10}(OH)_2$	0.0[a]	7.4
Glass	$SiAl_{0.358}Fe(II)_{0.189}Mg_{0.281}Ca_{0.264}Na_{0.079}K_{0.008}O_{3.315}$	0.25	7.4
Pyroxene	$CaAl_2SiO_6$	0.27	7.4
Plagioclase	$Ca_{0.7}Na_{0.3}Al_{1.7}Si_{2.3}O_8$	0.33	7.4
Forsterite	Mg_2SiO_4	0.13	7.4

Dissolution rate parameters

Mineral/glass	Acid mechanism			Neutral mechanism		Base mechanism		
	k_{25} (mol/m^2/s)[b]	E_a (KJ//mol)[b]	n (H^+)[b]	k_{25} (mol/m^2/s)	E_a (KJ/mol)	k_{25} (mol/m^2/s)	E_a (KJ/mol)	n (H^+)
Amorphous SiO_2	–	–	–	5.89×10^{-13}	74.5	–	–	–
Illite	1.95×10^{-13}	48.0	0.22	3.89×10^{-15}	48.0	3.89×10^{-15}	48.0	−0.13
Calcite	0.501	14.4	1.00	1.55×10^{-6}	23.5	3.31×10^{-4}	35.4	1.00
Siderite	9.77×10^{-4}	20.9	0.90	1.26×10^{-9}	62.8	–	–	–
Magnesite	4.17×10^{-7}	14.4	1.00	4.57×10^{-10}	23.5	6.02×10^{-6}	62.8	1.00
Montmorillonite	1.95×10^{-13}	48.0	0.22	3.89×10^{-15}	48.0	3.89×10^{-15}	48.0	−0.13
Glass	5.37×10^{-5}	39.7	1.01	–	–	1.00×10^{-11}	38.4	−0.26
Pyroxene	1.50×10^{-7}	78.0	0.70	1.07×10^{-12}	78.0	–	–	–
Plagioclase	1.35×10^{-8}	42.1	0.63	1.23×10^{-11}	45.2	–	–	–
Forsterite	1.41×10^{-7}	67.2	0.47	2.29×10^{-11}	79.0	–	–	–

[a] The PREEQC code uses a minute initial concentration for precipitating minerals (see Table 1 and text).
[b] k_{25} is the kinetic rate constant at 25 °C; E_a is the Arrhenius activation energy; n (H^+) is the reaction order with respect to H+.

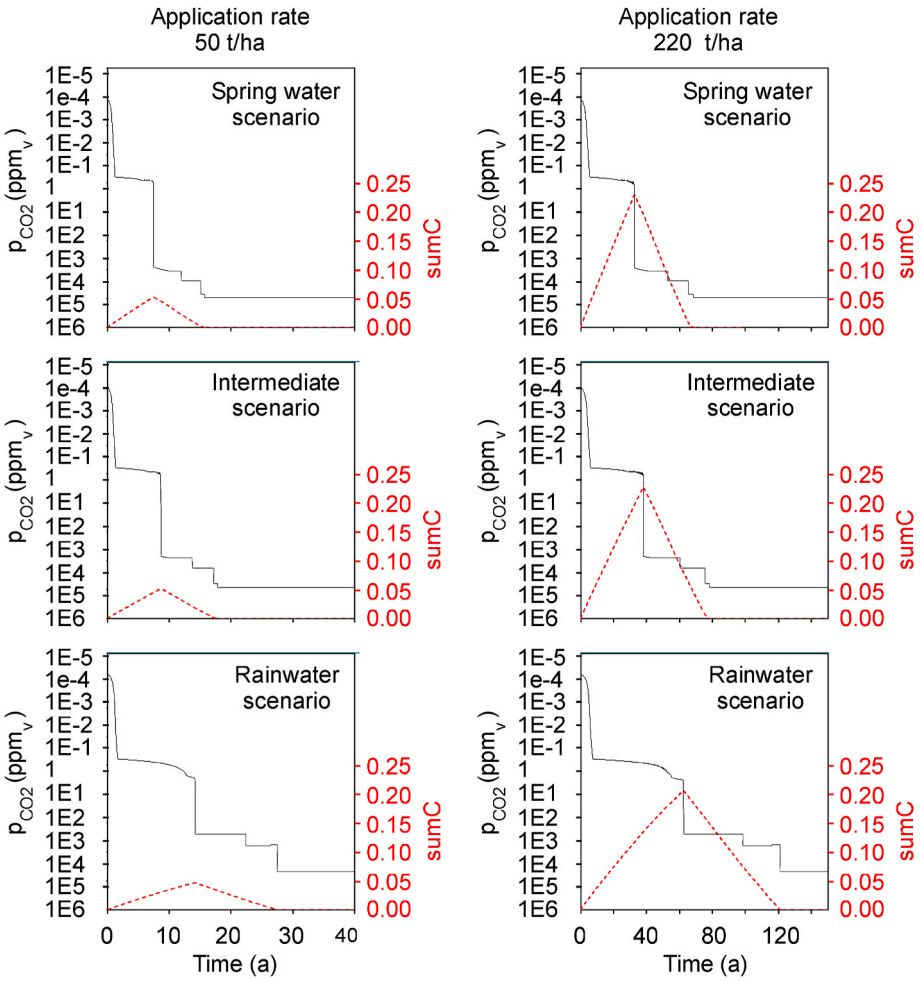

Fig. 1. Various model scenarios with CO_2 partial pressure (ppm_v; black solid line; vertical scale; text in black) and sumC value (moles of C per litre sequestered in solid mineral phases; red interrupted line; vertical scale text in red) plotted versus time. The infiltration rate is 1200 mm/a, and the basalt application rates are 50 and 220 t/ha (tonnes basalt per hectare).

or

$$I = 2.0R. \quad (2)$$

The initial concentration of solid components in contact with the reacting fluid (moles per litre of water) is derived from the composition of 50 or 220 tonnes basalt per hectare, corresponding to the minimum (Vienne et al., 2022) or maximum (Amann et al., 2020), respectively, tested experimentally. The rock grain density has the typical value of Columbia River basalt, U.S.A. (2.8 kg/dm^3; DOE 1982). The reactive surface area is 7.4 m^2/g, which is the maximum value tested experimentally (Kelland et al., 2020). Scoping calculations have shown that allowing for a relatively large surface area of clay minerals by multiplying the surface area by 10 has hardly any influence on recycling rates. Equally, multiplying or dividing the surface area of the remaining components by 3 has hardly any influence on recycling rates.

The glass fraction of basalt is 0.25, which is a typical value for Columbia River basalt, U.S.A., such as that used by Kelland et al. (2020). The proportion of the crystallized phases corresponds to the mineralogical composition of the basalt used by Pollyea and Rimstidt (2017) (Table 2). A volume fraction of 0.02, consisting of TiO_2 and P_2O_5 components, is neglected, i.e., assumed to be nonreactive. A simplified set of reaction products is used (Pollyea and Rimstidt, 2017): calcite, siderite, magnesite (i.e., carbonates representative of ankerite-dolomite solid solution; Reeder and Dollase, 1989), amorphous SiO_2, Ca-montmorillonite, Na-montmorillonite and illite (i.e., Al-silicates representative of a mixed-layer mineral solid solution; Meunier and Velde, 1989). There are no kinetic data for solid solutions; therefore, the available data for minerals with a fixed composition must be used. Basalt glass (Pollyea and Rimstidt, 2017) can only dissolve, whereas siderite (Knauss et al., 2005) and the remaining components (Palandri and Kharaka, 2004) dissolve and precipitate under kinetic constraints. Illite is assumed to have the same rate constants as montmorillonite. The precipitation rates equal dissolution rates.

The initial concentration of precipitating minerals is 0.0009 mol per litre of pores. This is the lowest concentration that allows convergence under optimal conditions, i.e., on UNIX-type platforms such as Intel Mac OS or LINUX.

2.1. Spring water scenario

The concentration of the major liquid components in the inlet fluid and initial reacting fluid (moles per litre of water) is the mean value calculated from a large number of major element analyses of groundwater springs in Brazilian Amazonia (47–165 analyses per element; Johnson et al., 2008, Table 3). These data are supplemented with minor element analyses of rainwater from southeastern Brazil (mean of 14 analysis; Oliveira et al., 2012, Table 3).

2.2. Rainwater scenario

The concentration of the liquid components in the inlet fluid and initial reacting fluid (moles per litre of water) is that of rainwater from

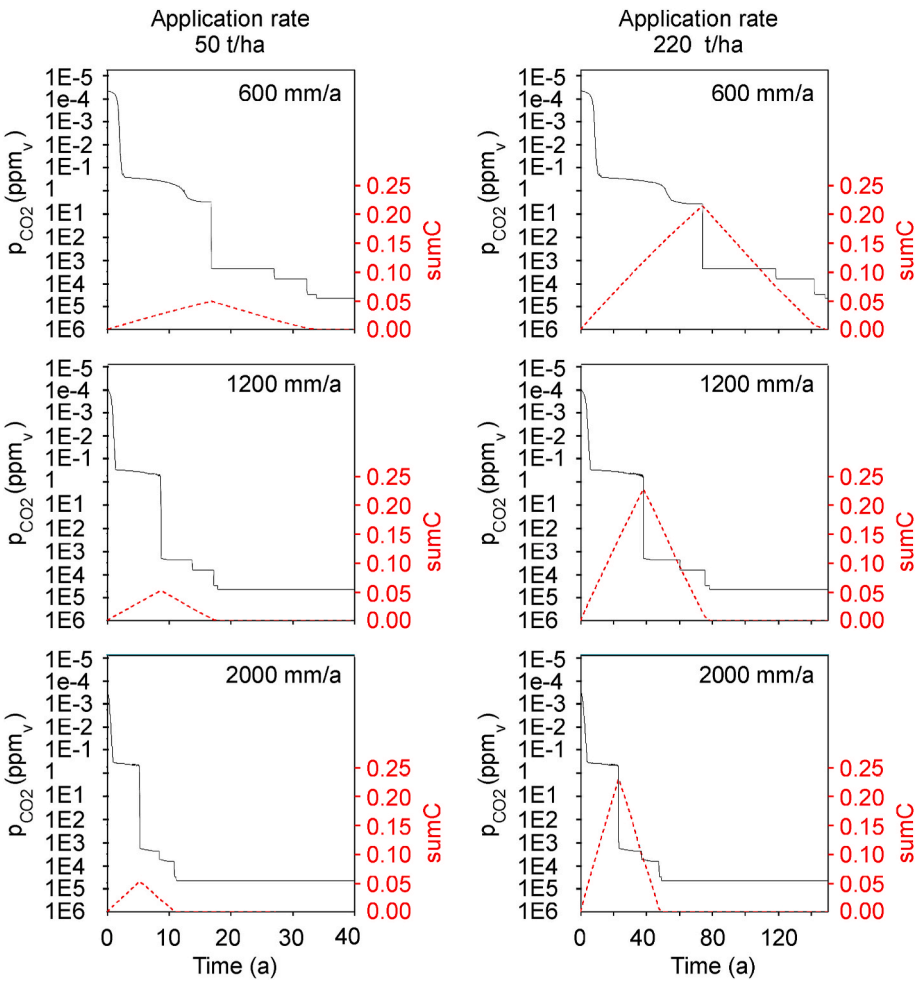

Fig. 2. Intermediate scenario with CO_2 partial pressure (ppm_v; black solid line; vertical scale; text in black) and sumC value (moles of C per litre sequestered in solid mineral phases; red interrupted line; vertical scale text in red) plotted versus time. The infiltration rates are 600, 1200 and 2000 mm/a, and the basalt application rates are 50 and 220 t/ha (tonnes basalt per hectare).

southeastern Brazil (mean of 14 analyses per element; Oliveira et al., 2012, Table 3).

2.3. Intermediate scenario

The intermediate scenario is meant to be a benchmark scenario. Neither the rainwater scenario nor the spring water scenario can be a realistic model of the real world because the reacting pore waters would have a mean composition in between these extremes. Ideally, the intermediate scenario would have a concentration of the liquid components in the inlet fluid and initial reacting fluid (moles per litre of water) corresponding to that of rainwater mixed with spring water at a ratio of 0.5:0.5. Due to convergence constraints of the PHREEQC program, the maximum mixing ratio that can be achieved is about 0.35:0.65. A mixing ratio of 0.3:0.7 is applicable to all models and is the basis of the intermediate scenario.

3. Results

The performance of the basalt reactor is monitored by variations in the CO_2 partial pressure (p_{CO2}) and concomitant sumC value (Figs. 1 and 2); sumC represents moles of solid C phases per litre of water formed from components of dissolving basalt and aqueous C species. The sumC value after the peak of CO_2 sequestration has been reached (critical sumC) and its corresponding CO_2 partial pressure (critical p_{CO2}) define the recycled CO_2 fraction (critical sumC divided by peak sumC; Fig. 3). The critical p_{CO2} is the atmospheric p_{CO2} (e.g., 420 ppm_v in 2023) of the receiving water courses in the case of water with p_{CO2} in equilibrium with the atmosphere. Most commonly, terrestrial surface waters are supersaturated with respect to atmospheric p_{CO2}. American rivers tend to have a higher degree of supersaturation than Asian streams. Generally, rivers in a warm climate zone have a higher degree of supersaturation than those in a cold climate zone (Zhang et al., 2017).

For a given critical p_{CO2}, the recycled fraction increases with increasing acidity and concentration of dissolved C in the water reacting with basalt, i.e., from the rainwater scenario through the intermediate scenario to the spring water scenario (Table 4). The influences of the infiltration rate and basalt application rate are minor. The lowest degree of recycling is achieved at the maximum infiltration rate (2000 mm/a) and minimum application rate (50 tonnes basalt per hectare) in the intermediate scenario (Table 5).

In the absence of useable data on the chemical composition of pore fluids in tropical soils, the intermediate scenario is taken as the reference scenario. The recycled CO_2 fraction is in the range of 0.18–1 in this benchmark scenario. Excluding the rapidly degassing 1st-order streams in Brazilian Amazonia (Johnson et al., 2008), the recycled fraction is in the range of 0.34–1. A benchmark is proposed with the mean p_{CO2} of 47 large rivers worldwide (3200 ppm_v; Cole and Caraco, 2001), which defines a recycling fraction in the narrow range of 0.34–0.43 in the benchmark scenario.

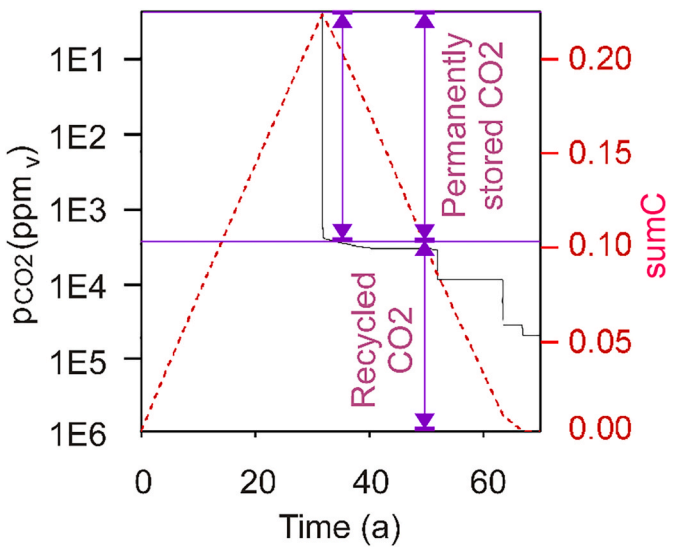

Fig. 3. Graphical scheme for visualizing the calculation of the CO_2 recycling rate after the peak of CO_2 sequestration has been reached. A sumC value (moles of solid C phases per litre) with its corresponding CO_2 partial pressure (p_{CO2}) defines the recycled fraction (sumC value divided by peak sumC). The CO_2 partial pressure (ppm_v) is shown as black solid line and a vertical scale with text in black. The sumC value (moles of solid C phases per litre) is shown as red interrupted line and a vertical scale with text in red. The explaining features are shown as violet text and lines.

4. Discussion and conclusion

The recycling of CO_2 originally sequestered in solid carbonate phases in basalt-amended fertilizer is a function of numerous variables. The variables modelled in this paper include.

- the pH and dissolved carbon concentration of the infiltrating fluids
- the infiltration rate
- the basalt application rate
- the degree of CO_2 supersaturation of the water courses that receive the pore fluids that have reacted with basalt.

Other factors like varying flow rates or parameters underlying precipitate dissolution kinetics are not included in the model because of lack of empirical or literature data.

The recycling rate decreases with increasing degree of supersaturation of the surface waters. CO_2 is less likely to be recycled to the atmosphere if the surface water–atmosphere system of the receiving streams favours supersaturation. The factors controlling supersaturation are incompletely known. Among the important variables are kinetics, within-stream mixing velocity and the ratio between the water surface and the water volume but it is not possible to establish a reasonable hierarchy of these variables (Finlay, 2003; Rasera et al., 2008; Alin et al., 2011; Raymond et al., 2013; Stets et al., 2017).

The reported recycling fractions referring to high-order streams (excluding first-order streams) span the range from 0.34 to 1. The dominant source of this variability is the p_{CO2} of soil waters and receiving streams. The p_{CO2} is a function of climate (tropical versus moderate). Another important factor may be the geographical location as far as the p_{CO2} of the receiving streams is concerned (America versus Asia). Note that basalt application rates (50–220 tonnes per hectare) and infiltration rates (600–2000 mm/a) only have a minor influence on the recycling fraction.

Most likely, CO_2 sequestered by basalt-amended fertilizer is at least partly recycled to the atmosphere under unfavourable conditions. These are high p_{CO2} and low pH of soil pore fluids in concert with a low degree of CO_2 supersaturation of the receiving streams or no supersaturation at all. On the one hand, rivers in a warm climate zone generally show a higher degree of supersaturation than those in a cold climate zone (Zhang et al., 2017). On the other hand, the soil pore fluids in a warm climate zone tend to be more acidic and tend to have a higher concentration of dissolved carbon than those in a cold climate zone (Brook et al., 1983; Kessler and Harvey, 2001). As a working hypothesis, it can be assumed that the negative and positive effects of climate cancel each other out. In other words, the recycling rate can be assumed to be independent of climate.

This paper does not consider the CO_2 emissions that are prevented from taking place during the period of carbonate minerals precipitation (ascending branch of the triangular-shaped time-sumC curve). Even in the theoretical case of zero net sequestration in the basalt-soil-river system, the gross CO_2 balance is positive when the prevented CO_2 emissions are included. The positive effect of prevented CO_2 emissions

Table 4
Fraction of recycled carbonates in various scenarios for basalt application rates of 50 and 220 tonnes basalt per hectare (t/ha) and an infiltration rate of 1200 mm/a (see text).

		Spring water scenario		Intermediate scenario		Rainwater scenario		
		50 t/ha	220 t/ha	50 t/ha	220 t/ha	50 t/ha	220 t/ha	
Reference sites [climate]	Mean pCO_2 (ppm_v)	Fraction of recycled carbonates (−)						Source
1st Order Streams (Amazonia) [tropical]	6106 ± 364 SE n = 84	0.42	0.39	0.40	0.40	0	0	Johnson et al. (2008)
Amazon River (Brazil) [tropical]	4350 ± 1900 SE	0.42	0.39	0.40	0.40	0	0	Richey et al. (2002)
47 large rivers (worldwide)	3200 n = 7965	0.82	0.91	0.40	0.41	0	0	Cole and Caraco (2001)
Xijiang River (China) [subtropical]	2600	0.96	1	0.40	0.41	0	0	Yao et al. (2007) quoted by Zhang et al. (2017)
Longchuan River (China) [subtropical]	2145 ± 2332 SD n = 244	1	1	0.97	0.97	0	0	Li et al. (2012)
Mississippi River [temperate]	1335 ± 129 SE n = 162	1	1	1	1	0.36	0.36	Dubois et al. (2010)
Yangtze River (China) [subtropical]	1297 ± 901 SD	1	1	1	1	0.36	0.36	Wang et al. (2007)
Lower Mekong River [tropical]	1090 ± 290 SD	1	1	1	1	0.36	0.36	Li et al. (2013)
York River (USA) [warm]	1070 ± 867 SD n = 99	1	1	1	1	0.36	0.36	Raymond et al. (2000)
Atmosphere (2008)	375	1	1	1	1	1	1	Johnson et al. (2008)

Table 5
Fraction of recycled carbonates in the intermediate scenario for basalt application rates of 50 and 220 tonnes basalt per hectare (t/ha) and infiltration rates of 600, 1200 and 2000 mm/a (see text).

		600 mm/a		1200 mm/a		2000 mm/a		
		50 t/ha	220 t/ha	50 t/ha	50 t/ha	220 t/ha	50 t/ha	
Reference sites [climate]	Mean pCO_2 (ppm_v)	Fraction of recycled carbonates (−)						Source
1st Order Streams (Amazonia) [tropical]	6106 ± 364 SE n = 84	0.34	0.34	0.40	0.40	0.18	0.41	Johnson et al. (2008)
Amazon River (Brazil) [tropical]	4350 ± 1900 SE	0.34	0.34	0.40	0.40	0.43	0.41	Richey et al. (2002)
47 large rivers (worldwide)	3200 n = 7965	0.34	0.34	0.40	0.41	0.43	0.41	Cole and Caraco (2001)
Xijiang River (China) [subtropical]	2600	0.34	0.34	0.40	0.41	0.43	0.41	Yao et al. (2007) quoted by Zhang et al. (2017)
Longchuan River (China) [subtropical]	2145 ± 2332 SD n = 244	1	1	0.97	0.97	0.78	0.97	Li et al. (2012)
Mississippi River [temperate]	1335 ± 129 SE n = 162	1	1	1	1	1	1	Dubois et al. (2010)
Yangtze River (China) [subtropical]	1297 ± 901 SD	1	1	1	1	1	1	Wang et al. (2007)
Lower Mekong River [tropical]	1090 ± 290 SD	1	1	1	1	1	1	Li et al. (2013)
York River (USA) [warm]	1070 ± 867 SD n = 99	1	1	1	1	1	1	Raymond et al. (2000)
Atmosphere (2008)	375	1	1	1	1	1	1	Johnson et al. (2008)

increases with decreasing p_{CO2} of the receiving streams. In other words, the positive and negative effects of river p_{CO2} partly cancel out. Thus, the shortcomings of a steady-state model, which does not consider seasonal variations of precipitation or chemistry of soil and river water, are less severe in a gross CO_2 balance model. However, such a model constitutes a highly complex system that is difficult to model considering the shortcomings of the relatively simple recycling model of this paper. E.g., the roadblocks to a gross balance model are land use change, soil erosion or basalt powder wind dispersion.

Basalt-amended fertilizer has a great advantage over competing lime-amended fertilizer. Both basalt and lime amendments are suitable for neutralizing acidic soils. In contrast to basalt, dissolving lime (calcite and dolomite) recycles CO_2 to the atmosphere at low soil pH (West and McBride, 2005; Biasi et al., 2008). In contrast to basalt, lime lacks important nutrients such as potassium, iron and phosphorus. Nevertheless, both basalt and lime amendments may have a positive influence on the chemistry of the receiving streams. Terrestrial water enriched in constituents of dissolved fertilizer amendments mixing with sea water may favour p_{CO2} reduction in the marine environment, thereby enhancing the process of recapturing atmospheric CO_2 in the ocean. These effects are difficult to model, and the uncertainties are enormous. It is not known to which degree lime reaches the potential of basalt with regard to reducing ocean acidification.

CRediT authorship contribution statement

Michael O. Schwartz: Writing – original draft.

Declaration of competing interest

The author has no competing interests.

Data availability

No data was used for the research described in the article.

Appendix A. Supplementary data

Supplementary data to this article can be found online at https://doi.org/10.1016/j.apgeochem.2024.105937.

References

Alin, S.R., et al., 2011. Physical controls on carbon dioxide transfer velocity and flux in low-gradient river systems and implications for regional carbon budgets. J. Geophys. Res. 116, 1–17.

Amann, T., et al., 2020. Enhanced weathering and related element fluxes - a cropland mesocosm approach. Biogeosciences 17, 103–119.

Anda, M., Shamshuddin, J., Fauziah, C.I., Omar, S.R.S., 2009. Dissolution of ground basalt and its effect on oxisol chemical properties and cocoa growth. Soil Sci. 174, 264–271.

Beerling, D.J., et al., 2020. Potential for large-scale CO_2 removal via enhanced rock weathering with croplands. Nature 583, 242–248.

Biasi, C., et al., 2008. Direct experimental evidence for the contribution of lime to CO_2 release from managed peat soil. Soil Biol. Biochem. 40, 2660–2669.

Brook, G.A., Folkoff, M.E., Box, E.O., 1983. A world model for soil carbon dioxide. Earth Surf. Process. Landforms 8, 79–88.

Cole, J.C., Caraco, N.F., 2001. Carbon in catchments: connecting terrestrial carbon losses with aquatic metabolism. Mar. Freshw. Res. 52, 101–110.

De Villiers, O.D.H., 1961. Soil rejuvenation with crushed basalt in Mauritius. Int. Sugar J. 63, 363–364.

Dietzen, C., Harrisona, R., Michelsen-Correac, S., 2018. Effectiveness of enhanced mineral weathering as a carbon sequestration tool and alternative to agricultural lime: an incubation experiment. Int. J. Greenh. Gas Control 74, 251–258.

DOE, 1982. Site Characterization Report for the Basalt Waste Isolation Project. US Department of Energy (DOE) DOE/. RL 82-3, vol. II.

Dubois, K.D., Lee, D., Veizer, J., 2010. Isotopic constraints on alkalinity, dissolved organic carbon, and atmospheric carbon dioxide fluxes in the Mississippi River. J. Geophys. Res. 115, 1–11.

Fan, Y., Miguez-Macho, G., 2010. Potential groundwater contribution to Amazon evapotranspiration. Hydrol. Earth Syst. Sci. 14, 2039–2056.

Finlay, J.C., 2003. Controls of streamwater dissolved inorganic carbon dynamics in a forested watershed. Biochemistry 62, 231–252.

Gillman, G.P., Burkett, D.C., Coventry, R.J., 2002. Amending highly weathered soils with finely ground basalt rock. Appl. Geochem. 17, 987–1001.

Grieger, G., 2020. Amazon Deforestation and EU-Mercosur Deal. European Parliamentary Research Service, 659311. https://www.europarl.europa.eu/thinktank/en/document.html?reference=EPRS_ATA, 2020.

Hartmann, J., Moosdorf, N., 2012. A new global lithological map database GLiM: a representation of rock properties at the Earth surface. G-cubed 13 (12), 1–37.

Hilf, H., 1938. Die Düngung mit Basaltabfällen (The fertilization with basalt waste). Forstarchiv 14, 93–101.

Johnson, M.S., et al., 2008. CO_2 efflux from Amazonian headwater streams represents a significant fate for deep soil respiration. Geophys. Res. Lett. 35, 1–5.

Kelland, M.E., et al., 2020. Increased yield and CO_2 sequestration potential with the C_4 cereal *Sorghum bicolor* cultivated in basaltic rock dust-amended agricultural soil. Global Change Biol. 26, 3658–3676.

Kessler, T.J., Harvey, C.F., 2001. The global flux of carbon dioxide into groundwater. Geophys. Res. Lett. 28, 279–282.

Knauss, K.G., Johnson, J.W., Steefel, C.I., 2005. Evaluation of the impact of CO_2, co-contaminant gas, aqueous fluid and reservoir rock interactions on the geologic sequestration of CO_2. Chem. Geol. 217, 339–350.

Lefebvre, D., et al., 2019. Assessing the potential of soil carbonation and enhanced weathering through life cycle assessment: a case study for Sao Paulo State, Brazil. J. Clean. Prod. 233, 468–481.

Li, S., et al., 2012. Daily CO_2 partial pressure and CO_2 outgassing in the upper Yangtze River basin: a case study of the Longchuan River, China. J. Hydrol. 466, 141–150.

Li, S., Lu, X.X., Bush, R.T., 2013. CO_2 partial pressure and CO_2 emission in the lower Mekong River. J. Hydrol. 504, 40–56.

Meunier, A., Velde, B., 1989. Solid solutions in I/S mixed-layer minerals and illite. Am. Mineral. 74, 1106–1112.

Oliveira, P.L., Figueiredo, B.R., Cardoso, A.A., 2012. Rainwater major and trace element contents in Southeastern Brazil: an assessment of a sugar cane region in dry and wet period. J. Braz. Chem. Soc. 23 (12), 1–9.

Palandri, J.L., Kharaka, Y.K., 2004. A Compilation of Rate Parameters of Water-Mineral Interaction Kinetics for Application to Geochemical Modeling. U.S. Geological Survey Open File Report 2004-1068.
Parkhurst, D.L., Appelo, C.A.J., 2013. Description of input and examples for PHREEQC version 3 - a computer program for speciation, batch-reaction, one-dimensional transport, and inverse geochemical calculations. U.S. Geological Survey Techniques and Methods book 6 chap. A43.
Pollyea, R.M., Rimstidt, J.D., 2017. Rate equations for modeling carbon dioxide sequestration in basalt. Appl. Geochem. 81, 53–62.
Rasera, M.F.F.L., Ballester, M.V.R., Krushe, A.V., 2008. Small rivers in the Southwestern Amazon and their role in CO_2 outgassing. Earth Interact. 12, 1–16.
Raymond, P.A., Bauer, J.E., Cole, J.J., 2000. Atmospheric CO_2 evasion, dissolved inorganic carbon production, and net heterotrophy in the York River estuary. Limnol. Oceanogr. 45, 1707–1717.
Raymond, P.A., et al., 2013. Global carbon dioxide emissions from inland waters. Nature 503, 355–359.
Reeder, R.J., Dollase, W.A., 1989. Structural variation in the dolomite-ankerite solid-solution series: an X-ray, Mössbauer, and TEM study. Am. Mineral. 74, 1159–1167.
Richey, J.E., et al., 2002. Outgassing from Amazonian rivers and wetlands as a large tropical source of atmospheric CO_2. Nature 416, 617–620.
Stets, E.G., et al., 2017. Carbonate buffering and metabolic controls on carbon dioxide in rivers. Global Biochemical Cycles 31, 663–667.
Strefler, J., Amann, T., Bauer, N., Kriegler, E., Hartmann, J., 2018. Potential and costs of carbon dioxide removal by enhanced weathering of rocks. Environ. Res. Lett. 13, 1–26.
Taylor, L.L., et al., 2015. Enhanced weathering strategies for stabilizing climate and averting ocean acidification. Nat. Clim. Change 6, 402–406.
Taylor, L.L., Beerling, D.J., Quegan, S., Banwart, S.A., 2017. Simulating carbon capture by enhanced weathering with croplands: an overview of key processes highlighting areas of future model development. Biol. Lett. 13, 1–8.
ten Berge, H.F.M., et al., 2012. Olivine weathering in soil, its effects on growth and nutrient uptake in Ryegrass (*Loium perenne* L.): a pot experiment. PLoS One 7 (8), e42098. https://doi.org/10.1371/journal.pone.0042098.
van Straaten, P., 2006. Farming with rocks and minerals: challenges and opportunities. An Acad. Bras Ciências 78, 731–747.
Vienne, A., et al., 2022. Enhanced weathering using basalt rock powder: carbon sequestration co-benefits and risks in a mesocosm study with *Solanum tuberosum*. Frontiers in Climate 4, 1–14.
Wang, F., et al., 2007. Human impact on the historical change of CO_2 degassing flux in River Changjiang. Geochem. Trans. 8, 1–10.
Wei, Z., et al., 2017. Revisiting the contribution of transpiration to global terrestrial evapotranspiration. Geophys. Res. Lett. 44, 2792–2801.
West, T.O., McBride, A.C., 2005. The contribution of agricultural lime to carbon dioxide emissions in the United States: dissolution, transport, and net emissions. Agric. Ecosyst. Environ. 108, 145–154.
Yao, G., et al., 2007. Dynamics of CO_2 partial pressure and CO_2 outgassing in the lower reaches of the Xijiang River, a subtropical monsoon river in China. Sci. Total Environ. 376, 255–266.
Zhang, T., et al., 2017. River sequesters atmospheric carbon and limits the CO_2 degassing in karst area, southwest China. Sci. Total Environ. 609, 92–101.